

NLRP3 deficiency protects against acetaminophen-induced liver injury by inhibiting hepatocyte pyroptosis

XINYING YUAN^{1*}, PENG CHEN^{1,2*}, XIAOYU LUAN¹, CHAOQUN YU¹, LONGYU MIAO¹,
YARU ZUO¹, ANXU LIU¹, TIANYI SUN¹ and GUOHU DI^{1,2}

¹Department of Special Medicine, School of Basic Medicine, Qingdao University; ²Institute of Stem Cell and Regenerative Medicine, School of Basic Medicine, Qingdao University, Qingdao, Shandong 266071, P.R. China

Received September 22, 2023; Accepted January 23, 2024

DOI: 10.3892/mmr.2024.13185

Abstract. Acetaminophen (APAP) overdose is the primary cause of drug-induced acute liver failure in numerous Western countries. NLR family pyrin domain containing 3 (NLRP3) inflammasome activation serves a pivotal role in the pathogenesis of various forms of acute liver injury. However, the cellular source for NLRP3 induction and its involvement during APAP-induced hepatotoxicity have not been thoroughly investigated. In the present study, hematoxylin and eosin staining was performed to assess histopathological changes of liver tissue. Immunohistochemistry staining (NLRP3, Caspase-1, IL-1 β , GSDMD and Caspase-3), western blotting (NLRP3, Caspase-1, IL-1 β , GSDMD and Caspase-3) and RT-qPCR (NLRP3, Caspase-1 and IL-1 β) were performed to assess the expression of NLRP3/GSDMD signaling pathway. TUNEL staining was performed to assess apoptosis of liver tissue. The serum expression levels of inflammatory factors (IL-6, IL-18, IL-1 β and TNF- α) were assessed using ELISA and inflammation of liver tissue was assessed using immunohistochemistry (Ly6G and CD68) and RT-qPCR (TNF- α , IL-6, M ϕ -1, Cxcl-1, Cxcl-2). A Cell Counting Kit-8 was performed to assess cell viability and apoptosis. Protein and gene expression were analyzed by western blotting (PCNA, CCND1) and RT-qPCR (*CyclinA2*, *CyclinD1* and *CyclinE1*). Through investigation of an APAP-induced acute liver injury model (AILI), the present study demonstrated that APAP overdose induced activation of NLRP3 and cleavage of gasdermin D (GSDMD) in hepatocytes, both *in vivo* and *in vitro*. Additionally, mice with hepatocyte-specific knockout of *Nlrp3* exhibited reduced liver injury and lower mortality following APAP intervention,

accompanied by decreased infiltration of inflammatory cells and attenuated inflammatory response. Furthermore, pharmacological blockade of NLRP3/GSDMD signaling using MCC950 or disulfiram significantly ameliorated liver injury and reduced hepatocyte death. Notably, hepatocyte *Nlrp3* deficiency promoted liver recovery by enhancing hepatocyte proliferation. Collectively, the present study demonstrated that inhibition of the NLRP3 inflammasome protects against APAP-induced acute liver injury by reducing hepatocyte pyroptosis and suggests that targeting NLRP3 may hold therapeutic potential for treating AILI.

Introduction

Drug-induced liver injury (DILI) is an adverse drug reaction that can result in acute liver failure (ALF) or even death. In developed nations, acetaminophen (APAP) overdose has become the leading cause of ALF and may require liver transplantation (1-3). In an overdose, APAP is transformed by cytochrome P450 into the toxic metabolite N-acetyl-p-benzoquinone imide (NAPQI) that causes hepatic glutathione depletion. N-acetylcysteine remains the only clinically authorized treatment for APAP overdose (4); however, its efficiency is significantly limited by its narrow therapeutic window and adverse effects (5). Therefore, understanding the mechanisms of APAP-induced cell death and identifying novel therapeutic targets are needed to treat APAP-induced liver injury (AILI).

The pathological process of AILI can be divided into three stages: Injury initiation, injury progression and liver recovery (6). Initially, accumulated NAPQI results in an overproduction of reactive oxygen species and mitochondrial dysfunction, which ultimately triggers hepatocyte necrosis and apoptosis (7). Subsequently, necrotic hepatocytes release damage-associated molecular patterns such as high-mobility group box 1 protein and DNA fragments, which lead to recruitment and activation of inflammatory cells like monocytes and neutrophils at site of injury (8,9). Finally, compensatory hepatocellular proliferation is initiated with hepatocytes surrounding the necrotic area replacing dead cells (10).

The NLR family pyrin domain containing 3 (NLRP3) inflammasome is one of the most extensively studied upstream activators of pyroptosis (11). Activation of NLRP3 leads to the

Correspondence to: Professor Guohu Di, Department of Special Medicine, School of Basic Medicine, Qingdao University, 308 Ningxia Road, Qingdao, Shandong 266071, P.R. China
E-mail: diguohu@qdu.edu.cn

*Contributed equally

Key words: NLR family pyrin domain containing 3, acetaminophen, pyroptosis, gasdermin D, liver regeneration

assembly of a protein complex (including NLRP3 oligomers and ASC) responsible for binding and cleaving caspase-1, which in turn generates the cleaved gasdermin D (GSDMD) N-terminal fragment (GSDMD-N) and forms pores in the cell membrane to induce pyroptosis, as well as releasing proinflammatory cytokines IL-1 β and IL-18 (12-14). Numerous studies have reported that NLRP3 activates pyroptosis in various liver diseases (15-18). However, the role of NLRP3 during APAP overdose has not been elucidated. Recent studies have demonstrated that pyroptosis occurs in APAP-induced liver injury through caspase-1 cleavage and GSDMD activation in both hepatocytes and Kupffer cells (19,20). Furthermore, it has been demonstrated that deficiency or knock-down of NLRP3 reduces the pyroptotic parameters and partially rescues APAP hepatotoxicity in mice (21,22). However, it has also been suggested that NLRP3 activation is not essential for APAP-induced liver injury (23,24). Nevertheless, further investigation is required to elucidate the relevance of NLRP3-mediated pyroptosis in APAP-induced hepatotoxic processes.

The present study aimed to investigate the effect of NLRP3 inflammasome during AILI. Moreover, the present study aimed to evaluate the therapeutic effects of NLRP3 and GSDMD inhibition in AILI both *in vivo* and *in vitro*.

Materials and methods

Animals and animal models. A total of 110 C57BL/6, 28 *Nlrp3^{fl/fl}* mice and 28 *Nlrp3^{Δhep}* mice were used. C57BL/6 male mice (8-week-old) weighing 20-22 g, were purchased from Beijing Vital River Laboratory Animal Technology Co., Ltd. (Charles River Laboratories). *Alb-iCre* (strain no. T003814) and *B6JNju;B6NNju-Nlrp3 (flper)^{tm1/Nju} [Nlrp3 locus of X-over P1 (Nlrp3^{loxP} or Nlrp3^{fl/fl})]* (strain no. T001231,) mice were purchased from GemPharmatech Co., Ltd. Hepatocyte-specific *Nlrp3* knockout mice (*Albcre⁺Nlrp3^{loxP/loxP}*, *Nlrp3^{Δhep}*) were generated by crossing the *Nlrp3^{loxP}* mice with *Alb-cre* mice and the mice were backcrossed for at least 10 generations on a C57BL/6 background. Male mice (age, 8 weeks old, 20-22 g) were used for the experiments. The mice were raised in a standard room with controlled humidity (55-60%) and temperature (23-25°C) under a 12 h light/dark cycle with *ad libitum* access to food and water. All mice received two daily health observations including water and food intake, weight and general assessment of animal activity. The study employed humane endpoints according to AVMA Guidelines for the Euthanasia of Animals (<https://www.avma.org/resources-tools/avma-policies/avma-guidelines-euthanasia-animals>), including when the mice showed an inability to obtain food or water on their own, had a weight loss of >20% of their starting body weight, difficulty moving, were depressed in the absence of anesthesia, or their body temperature was persistently below 37°C. All animal experiments were performed in accordance with the regulations of the ARRIVE guidelines and approved by The Ethics Committee Medical College of Qingdao University (Qingdao, China; approval no. QDU-AEC-2022310).

The APAP-induced liver injury model was established as previously described, with minor modifications (25). Briefly, 25 mg/ml APAP solution was prepared by dissolving APAP (Beijing Solarbio Science & Technology Co., Ltd.) in pyrogen-free phosphate-buffered saline (PBS) at 60°C and

cooled to 37°C before injection. The mice were fasted for 15-17 h and then intraperitoneally (IP) injected with a single dose of 300 mg/kg of APAP (sublethal dose; n=5 per group) or 500 mg/kg (lethal dose; n=10 per group). To evaluate the therapeutic effects of NLRP3 and GSDMD inhibition, NLRP3 inhibitor MCC950 (TargetMol Chemicals Inc.) was administered IP into mice at 50 mg/kg 2 h after APAP and GSDMD inhibitor disulfiram (DSF; TargetMol Chemicals Inc.) was administered IP into mice at 50 mg/kg 4 and 24 h before APAP (n=5 per group), with PBS or vehicle (sesame oil) as control group respectively. At 0, 6, 12, 24, 36 or 48 h, the mice were euthanized using 5% inhalational isoflurane for >3 min and death was verified by a lack of heartbeat and breathing. Liver tissue and serum samples were harvested for subsequent experiments.

Survival assays. The survival rates of *Nlrp3^{fl/fl}* and *Nlrp3^{Δhep}* mice were evaluated within 72 h after 500 mg/kg APAP treatment (lethal dose; n=10 per group) as previously described (26). Mice were housed under pathogen-free conditions and were monitored every 6 h with free access to food and water. All of the mice were euthanized at the end of the study.

Cell culture and treatment. Mouse primary hepatocytes were isolated from C57BL/6 mice (n=5), *Nlrp3^{fl/fl}* and *Nlrp3^{Δhep}* mice (n=3) as previously described by two-step perfusion methods with minor modifications (27,28). In brief, the liver was perfused with Hank's Balanced Salt Solution (Wuhan Servicebio Technology Co., Ltd.) containing EGTA (Beijing Solarbio Science & Technology Co., Ltd.) and digested with collagenase type IV (Gibco; Thermo Fisher Scientific, Inc.). Then, the liver was dissolved in residual digestive fluid and filtered with a 100 μ m cell strainer. Hepatocytes were obtained by low speed centrifugation (100 x g) for 2 min at 4°C. Cell culture plates were coated with 0.03 mg/ml rat tail collagen I 2 h in advance at room temperature and washed three times with sterile PBS before use. The cells were seeded onto 6-well or 96-well plates with 8x10⁴ cells/ml precoated with rat tail tendon collagen I (Shengyou Biotechnology Co., Ltd.). After overnight incubation, the cells were treated with 1, 2.5, 5 and 10 mM APAP for 12 h at 37°C.

The α mouse liver 12 (AML12) cell line was purchased from The Cell Bank of Type Culture Collection of The Chinese Academy of Sciences. The cells were cultured in DMEM/F12 (1:1) (Gibco; Thermo Fisher Scientific, Inc.) medium containing 10% fetal bovine serum (Shanghai ExCell Biology, Inc.), Insulin-Transferrin-Selenium (Beyotime Institute of Biotechnology) and 40 ng/ml dexamethasone (MilliporeSigma) with 5% CO₂ at 37°C. Upon reaching a confluency of 70 to 80%, the cells were incubated with 1, 5, 10 and 20 mM APAP for 24 h, subsequently total protein and RNA were extracted for western blotting and reverse transcription-quantitative PCR (RT-qPCR) respectively.

Cell Counting Kit-8 (CCK-8) assay. To investigate the therapeutic effects of NLRP3 and GSDMD inhibition *in vitro*, AML12 cells were seeded onto 96-well plates at a density of 1,000 cells per well, 0, 1, 5, 10 μ M MCC950 or 0, 1, 2.5, 5 μ M DSF were administrated to the AML12 cell complete medium, with or without 10 mM APAP. To evaluate the toxicity of APAP

Table I. Gene-specific primers used in reverse transcription-quantitative PCR.

| Gene | Accession no. | Direction | Primer sequence, 5'-3' |
|----------------------------------|----------------|-----------|----------------------------|
| <i>m-Gapdh</i> | NM_001289726.1 | Forward | GCCACCCAGAAGACTGTGGAT |
| | | Reverse | GGAAGGCCATGCCAGTGA |
| <i>m-Nlrp3</i> | NM_145827.4 | Forward | CTGCGGACTGTCCCATCAAT |
| | | Reverse | AGGTTGCAGAGCAGGTGCTT |
| <i>m-Caspase1</i> | NM_009807.2 | Forward | CTGGGACCCTCAAGTTTTGC |
| | | Reverse | CCCTCGGAGAAAGATGTTGAAA |
| <i>m-Il-1β</i> | NM_008361.4 | Forward | CTTTCCCGTGGACCTTCCA |
| | | Reverse | CTCGGAGCCTGTAGTGCAGTT |
| <i>m-Tnf-α</i> | NM_013693.3 | Forward | ACAAGGCTGCCCCGACTAC |
| | | Reverse | TGGGCTCATACCAGGGTTTG |
| <i>m-Il-6</i> | NM_031168.2 | Forward | ACCACTCCCAACAGACCTGTCT |
| | | Reverse | CAGATTGTTTTCTGCAAGTGCAT |
| <i>m-Mcp-1</i> | NM_011333.3 | Forward | CAGCAAGATGATCCCAATGAGTAG |
| | | Reverse | TTTTTAATGTATGTCTGGACCCATTC |
| <i>m-Cxcl-1</i> | NM_008176.3 | Forward | CGCTTCTCTGTGCAGCGCTGCTGCT |
| | | Reverse | AAGCCTCGCGACCATTCCTTGAGT |
| <i>m-Cxcl-2</i> | NM_009140.2 | Forward | CCTGGTTCAGAAAATCATCCA |
| | | Reverse | CTCCGTTGAGGGACAGC |
| <i>m-CyclinA2</i> | NM_009828.3 | Forward | TCAAGACTCGACGGGTTGCT |
| | | Reverse | GCTCAGCTGGCCTCTTCTGA |
| <i>m-CyclinD1</i> | NM_001379248.1 | Forward | TGCTGCAAATGGAAGTCTT |
| | | Reverse | CCACAAAGGTCTGTGCATGCT |
| <i>m-CyclinE1</i> | NM_007633.2 | Forward | TGTTACAGATGGCGCTTGCT |
| | | Reverse | ACCTCACCCGTGTCGTTGAC |

on hepatocytes, cell viability was measured using a CCK-8 assay (Shanghai Yeasen Biotechnology Co., Ltd.). Briefly, 10 μ l of CCK-8 solution was added to each well and incubated for 1 h at 37°C. Absorbance at 450 nm was measured by SpectraMax Absorbance Reader (Molecular Devices, LLC).

RT-qPCR. Total RNA was extracted from liver tissue, primary hepatocytes or AML12 cells using FastPure Cell/Tissue Total RNA Isolation kit (Vazyme Biotech Co., Ltd.). RNA was reverse transcribed into cDNA using specific primers for *Nlrp3*, *Caspase 1*, *Il-1 β* , *Tnf- α* , *Il-6*, *Mcp-1*, *Cxcl-1*, *Cxcl-2*, *CyclinA2*, *CyclinD1* and *CyclinE1* (Table I) using the PrimeScript First Strand cDNA Synthesis kit (Takara Biotechnology Co., Ltd.) according to the manufacturer's protocol. As previously described (29), qPCR was performed using SYBR Premix Ex Taq (Vazyme Biotech Co., Ltd.) on a CFX96 Real-Time Systems (Bio-Rad Laboratories, Inc.). The thermocycling conditions were as follows: Pre-incubation at 95°C for 2 min; amplification at 95°C for 10 sec and 60°C for 20 sec, followed by 40 cycles; melting curve at 65°C for 5 sec and 95°C for 15 sec. The mRNA levels were quantified using the 2^{- $\Delta\Delta$ C_q} method and normalized to the internal reference gene GADPH (30).

Western blotting. Total protein from liver tissue, primary hepatocytes or AML12 cells was extracted using RIPA buffer (Wuhan Servicebio Technology Co., Ltd.) as

described previously (31). BCA Protein Assay kit (Epizyme; ZJ102) to confirm the protein concentration. Briefly, the protein samples (40 μ g) were separated by 7.5, 10 and 12.5% sodium dodecyl sulfate-polyacrylamide gel electrophoresis and transferred to a polyvinylidene fluoride membrane (MilliporeSigma). After blocking with 5% skimmed milk powder for an hour at room temperature, the membranes were incubated with primary antibodies including: NLRP3 (1:1,000; AG-20B-0014-C100; Adipogen Life Sciences, Inc.), IL-1 β (1:1,000; A11369; ABclonal Biotech Co., Ltd.), Caspase-1 (1:1,000; A0964; ABclonal Biotech Co., Ltd.), GSDMD (1:1,000; cat. no. AF4012; Affinity Biosciences), β -actin (1:1,000; AC026; ABclonal Biotech Co., Ltd.), Caspase-3 (1:1,000; 9662S; Cell Signaling Technology, Inc.), PCNA (1:1,000; AF0239; Affinity Biosciences), CyclinD1 (1:1,000; A0310; ABclonal Biotech Co., Ltd.) at 4°C overnight. Next day, these membranes were washed three times using Tris-buffered saline with 0.1% Tween-20 for ten minutes each and then incubated with Goat Anti-Mouse IgG (H+L) HRP or Goat Anti-Rabbit IgG (H+L) HRP (1:4,000; S0002; S0001; Affinity Biosciences,) for 1 h at room temperature. Finally, protein bands were washed three times again and visualized using an ultra sensitive chemiluminescence assay kit (Shanghai Epizyme Biotech Co., Ltd.) and imaged using an automatic chemiluminescence image analysis system (Tanon Science and Technology Co., Ltd.). Protein levels were quantified using ImageJ software

(version 1.43; National Institutes of Health) with β -actin as the loading control.

Biochemical analysis and ELISA assay. Blood serum aspartate transaminase (AST) and serum alanine aminotransferase (ALT) levels in mice were measured using a Chemray 800 automatic biochemical analyzer (Rayto Life and Analytical Sciences Co., Ltd.) according to the manufacturer's instructions (S03040; S03030; Rayto Life and Analytical Sciences Co., Ltd.). Additionally, levels of inflammatory cytokines IL-6, IL-18, IL-1 β and TNF- α were measured using mouse interleukin-6 (IL-6) ELISA kit (ml098430); mouse interleukin-18 (IL-18) ELISA kit (ml002294); mouse interleukin-1 β (IL-1 β) ELISA kit (ml098416); mouse tumor necrosis factor- α (TNF- α) ELISA kit (ml002095) (Shanghai Enzyme-linked Biotechnology Co., Ltd.) according to the manufacturer's instructions. The absorbance values were measured at 450 nm using a SpectraMax Absorbance Reader (Molecular Devices, LLC).

Immunohistochemical staining (IHC) and TUNEL assay. Histological sectioning and IHC were performed as previously described (32). Briefly, liver samples from the left lateral lobes of mice were fixed with 4% paraformaldehyde (Wuhan Servicebio Technology Co., Ltd., G1101) for 24 h at room temperature and embedded in paraffin or optimal cutting temperature (OCT) compound (Wuhan Servicebio Technology Co., Ltd.) and stored at -80°C. The paraffin was sliced into 5 μ m sections and frozen OCT compound samples were sliced into 8 μ m sections. Sections were hematoxylin and eosin (H&E) stained to examine the pathological changes in liver tissue after deparaffinization and dehydration through descending ethyl alcohol. For IHC, the sections were subjected to antigen retrieval by microwaving in citrate buffer (pH 6.0, Biogenex, CA) for 20 min at 99–100°C. After washing with PBS for 15 min, the sections were incubated with 3% hydrogen peroxide for 10 min at room temperature. IHC was carried out by incubating the sections with antibodies including: NLRP3 (1:200; DF7834; Affinity Biosciences), IL-1 β (1:200; ab9722; Abcam), Caspase-1 (1:200; ab207802; Abcam), GSDMD (1:200; AF4012; Affinity Biosciences), PCNA (1:200; cat. no. ab92552; Abcam), Ki67 (1:200; ab15580; Abcam), CD68 (1:200; GB113109; Wuhan Servicebio Technology Co., Ltd.), Ly6G (1:200; GB11229; Wuhan Servicebio Technology Co., Ltd.) and Caspase-3 (1:200; 9662S; Cell Signaling Technology, Inc.) at 4°C overnight. Next day, according to the manufacturer's instructions for immunochromogenic reagent (EliVision plus mouse/rabbit) (KIT9901, Maixing Company, China), the sections were incubated with R1 (reaction enhancement solution) for 20 min, and then incubated with R2 (HRP-conjugated anti-mouse/rabbit IgG polymer) in the dark for 30 min at room temperature. Finally, the sections were stained with DAB chromogenic kit (Wuhan Servicebio Technology Co., Ltd.) for 2 min at room temperature. The sections were images of the sections were captured under an BX50 light microscope (Olympus Corporation).

The frozen sections were subjected to TUNEL staining using a TUNEL kit (Shanghai Yeasen Biotechnology Co., Ltd.), following the manufacturer's instructions. Briefly, the sections were fixed with 4% paraformaldehyde at room temperature for 30 min. After washing with PBS for 30 min, Proteinase K (20 μ g/ml) were incubated for 10 min at room

temperature and TDT incubation buffer were incubated at 4°C overnight. Subsequently, nuclei were counterstained with 2 μ g/ml 4',6-diamidino-2-phenylindole (Beyotime Institute of Biotechnology) for 5 min at room temperature. The sections were sealed with PBS. The TUNEL-positive cells were visualized under a fluorescence microscope (Olympus Corporation) and 5 numbers of field were calculated.

Statistical analysis. All experiments were conducted at least three times, and statistical analyses were performed using GraphPad Prism 8.0 software (Dotmatics). Differences between groups were assessed using an unpaired Student's t-test for two groups or one-way ANOVA followed by Tukey's post hoc test for multiple groups. Survival curves were compared using the log-rank (Mantel-Cox) test. $P < 0.05$ was considered to indicate a statistically significant difference.

Results

APAP overdose induces NLRP3 activation in hepatocytes in vivo and in vitro. As previously described (25), an APAP-induced liver injury mouse model was established by IP injection of a single dose of 300 mg/kg APAP. APAP treatment resulted in liver injury characterized by increased hepatic necrosis (Fig. 1A and B) and elevated serum ALT (Fig. 1C) and AST levels (Fig. 1D). To investigate the potential role of NLRP3 activation in APAP-induced hepatotoxicity, expression levels of NLRP3 in AILI mice were examined. IHC demonstrated an increase in NLRP3, Caspase-1, IL-1 β and GSDMD in mice liver after APAP treatment compared with control group (sham) (Fig. 1E). Likewise, increased protein levels of NLRP3, cleaved IL-1 β and GSDMD were shown by western blotting compared with the control group (sham) (Fig. 1F). Additionally, APAP treatment increased the levels of proinflammatory cytokines IL-1 β (Fig. 1G) and IL-18 (Fig. 1H) in mouse serum compared with 0 h, indicating the activation of NLRP3 and GSDMD. To determine the cellular source of NLRP3 expression after 24 or 48 h post-treatment with APAP, mouse liver parenchymal cells were isolated for western blotting, which showed increased levels of NLRP3, cleaved caspase-1, cleaved IL-1 β and GSDMD-N at 24 h post APAP treatment (Fig. 1I).

To investigate whether APAP overdose induces NLRP3 activation in mouse hepatocytes *in vitro*, AML12 cells and primary hepatocytes were subjected to APAP treatment for 24 and 12 h, respectively. These results showed that both cell types exhibited dose-dependent decrease in cell viability with APAP treatment (Fig. 2A). Likewise, APAP treatment increased the mRNA expression levels of *Nlrp3* (Fig. 2B), *Caspase-1* (Fig. 2C) and *Il-1 β* (Fig. 2D) in AML12 cells and primary hepatocytes compared with the control. Furthermore, the protein levels of NLRP3 and the active fragments of pyroptosis-related proteins, cleaved caspase-1, cleaved IL-1 β and GSDMD-N were elevated upon APAP treatment in both AML12 and primary hepatocytes compared with the control (Fig. 2E–F). Taken together, the aforementioned findings suggested that APAP overdose triggers NLRP3 activation leading to hepatocyte pyroptosis both *in vivo* and *in vitro*.

Hepatic Nlrp3 deficiency protects mice from APAP-induced acute liver injury. As NLRP3 is crucial for APAP-induced

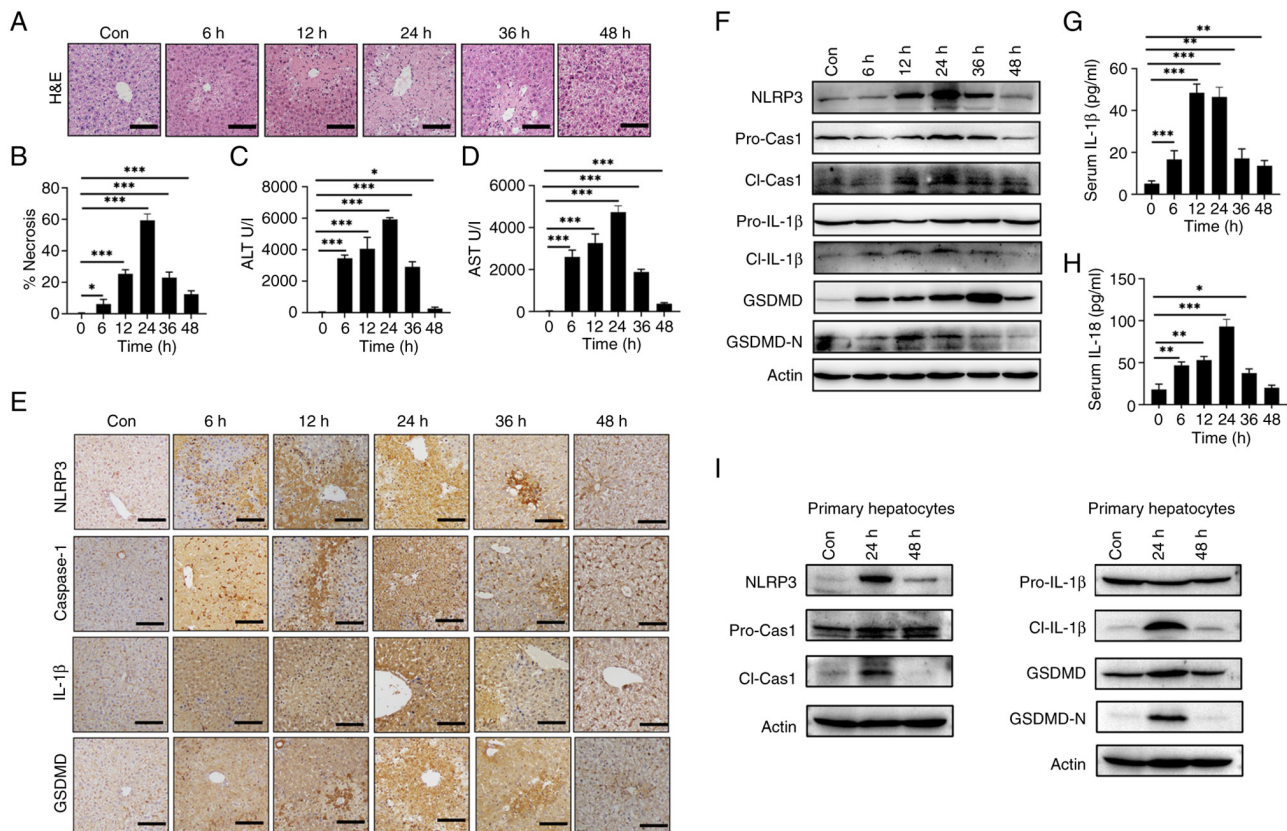


Figure 1. APAP overdose induces hepatic NLRP3 activation in mice. C57BL/6 mice were intraperitoneally injected with 300 mg/kg APAP at the indicated time points (n=5). The histopathological dynamic changes of liver tissues shown by (A) H&E staining in liver tissues and (B) statistical quantification of hepatic necrosis area. Serum levels of (C) ALT and (D) AST. (E) IHC staining of NLRP3, caspase-1, IL-1 β and GSDMD in liver tissues. (F) Western blotting of NLRP3, pro-cas-1, cl-cas-1, pro-IL-1 β , cl-IL-1 β , GSDMD and GSDMD-N in liver tissues. Serum levels of (G) IL-1 β and (H) IL-18. (I) Mouse liver parenchymal cells were isolated after 24 or 48 h post-treatment with APAP for western blotting of NLRP3, pro-cas-1, cl-cas-1, pro-IL-1 β , cl-IL-1 β , GSDMD and GSDMD-N. Data are presented as the mean \pm SD. * P <0.05, ** P <0.01, *** P <0.001. pro-cas-1, pro-caspase-1; cl-cas-1, cl-caspase-1; GSDMD, gasdermin D; GSDMD-N, cleaved GSDMD N-terminal fragment; cl-IL-1 β , cleaved IL-1 β ; APAP, acetaminophen; NLRP3, NLR family pyrin domain containing 3; ALT, alanine aminotransferase; AST, aspartate transaminase; con, control; IHC, immunohistochemistry.

hepatocyte pyroptosis, *Nlrp3^{Δhep}* mice were generated by crossing *Nlrp3^{fl/fl}* mice with *Albcre+* mice. Western blotting confirmed the specific knockout of *Nlrp3* in hepatocytes and not in non-parenchymal cells (Fig. 3A). To investigate the impact of hepatic *Nlrp3* deficiency on APAP-induced liver injury, AILI models were created using *Nlrp3^{fl/fl}* and *Nlrp3^{Δhep}* mice. Survival assays were conducted through IP injection of a lethal dose (500 mg/kg) of APAP, revealing significantly lower mortality in *Nlrp3^{Δhep}* mice compared with *Nlrp3^{fl/fl}* mice (Fig. 3B). Liver damage was assessed by injecting 300 mg/kg APAP and measuring alanine aminotransferase (ALT) (Fig. 3C) and aspartate aminotransferase (AST) levels (Fig. 3D), as well as the level of necrosis in liver tissue (Fig. 3E), all of which showed significant reductions in *Nlrp3^{Δhep}* mice when compared with *Nlrp3^{fl/fl}* mice. Consistently, livers from *Nlrp3^{Δhep}* mice exhibited lower TUNEL-positive staining after APAP treatment compared with the *Nlrp3^{fl/fl}* mice (Fig. 3F). These findings indicate that hepatic blockade of NLRP3 not only protects against APAP-induced liver injury but also improves survival.

Hepatic *Nlrp3* deficiency attenuates hepatic inflammatory response to APAP overdose. During the pathogenesis of AILI, the immune response serves a crucial role, and a timely decrease in inflammation is believed to be important in repairing acute

liver injury in mice (33). To investigate whether the protective effect from liver injury in *Nlrp3^{Δhep}* mice is related to hepatic decrease in inflammation, the levels of inflammation between the two groups were analyzed after treatment with 300 mg/kg APAP. IHC staining for Ly6G and CD68, which represent infiltration of liver neutrophils and macrophages, respectively, were significantly reduced in *Nlrp3^{Δhep}* mice at 24 and 48 h compared with the *Nlrp3^{fl/fl}* mice (Fig. 4A). Furthermore, there was a significant decrease in mRNA expression levels of pro-inflammatory cytokines *Tnf- α* and *Il-6* at 24 h, and for *Il-1 β* at both 24 and 48 h post-APAP treatment compared with the *Nlrp3^{fl/fl}* mice. Furthermore, a significant decrease in proinflammatory chemokine mRNA levels of *Mcp-1* and *Cxcl-1* at 24 h and of *Cxcl-2* at 24 and 48 h post APAP treatment was observed in *Nlrp3^{Δhep}* mice compared with *Nlrp3^{fl/fl}* mice (Fig. 4B).

Additionally, compared with *Nlrp3^{fl/fl}* mice, significantly decreased protein levels of TNF- α (Fig. 4C), IL-6 (Fig. 4D) at 24 and 48 h, and IL-1 β (Fig. 4E) at 24 h post-APAP treatment were measured in *Nlrp3^{Δhep}* serum samples. These findings suggest that ablation of hepatic NLRP3 may alleviate APAP-induced liver injury by reducing inflammation.

NLRP3/GSDMD inhibition alleviates APAP-induced acute liver injury. To assess the therapeutic potential of NLRP3

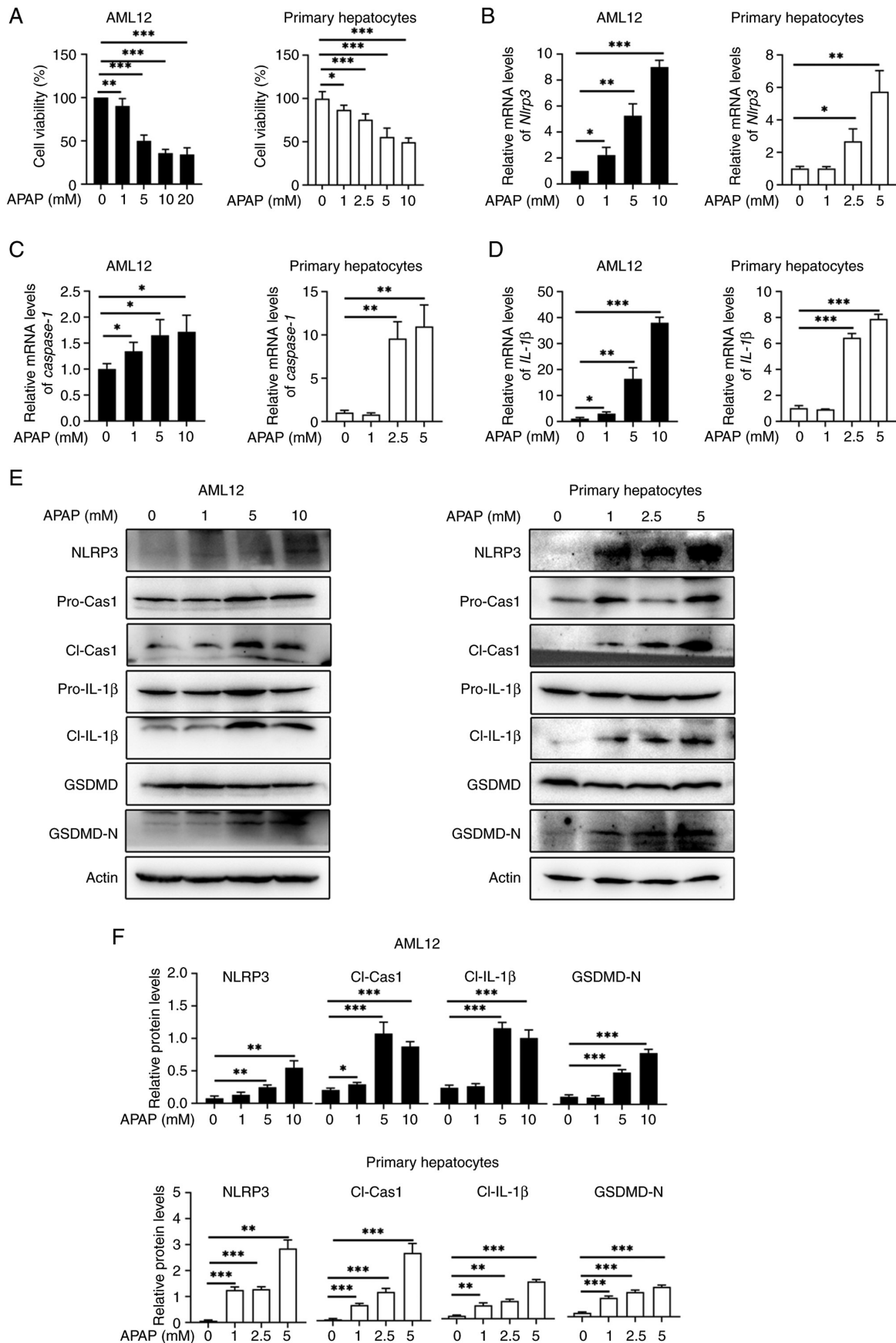


Figure 2. APAP induces NLRP3 activation and pyroptosis in hepatocytes *in vitro* (n=3). AML12 cells and mouse primary hepatocytes were stimulated with different concentrations of APAP for 24 h or 12 h. (A) Viability of both cell types. RT-qPCR analysis of (B) *Nlrp3*, (C) *caspase-1* and (D) *Il-1 β* in these two cell types. (E) Western blotting and (F) quantification of NLRP3, pro-cas-1, cl-cas-1, pro-IL-1 β , cl-IL-1 β , GSDMD and GSDMD-N in both cell types. Data are presented as the mean \pm SD. *P<0.05, **P<0.01, ***P<0.001. pro-cas-1, pro-caspase-1; cl-cas-1, cl-caspase-1; GSDMD, gasdermin D; GSDMD-N, cleaved GSDMD N-terminal fragment; APAP, acetaminophen; NLRP3, NLR family pyrin domain containing 3; ALT, alanine aminotransferase; AST, aspartate transaminase; RT-qPCR, reverse transcription-quantitative PCR.

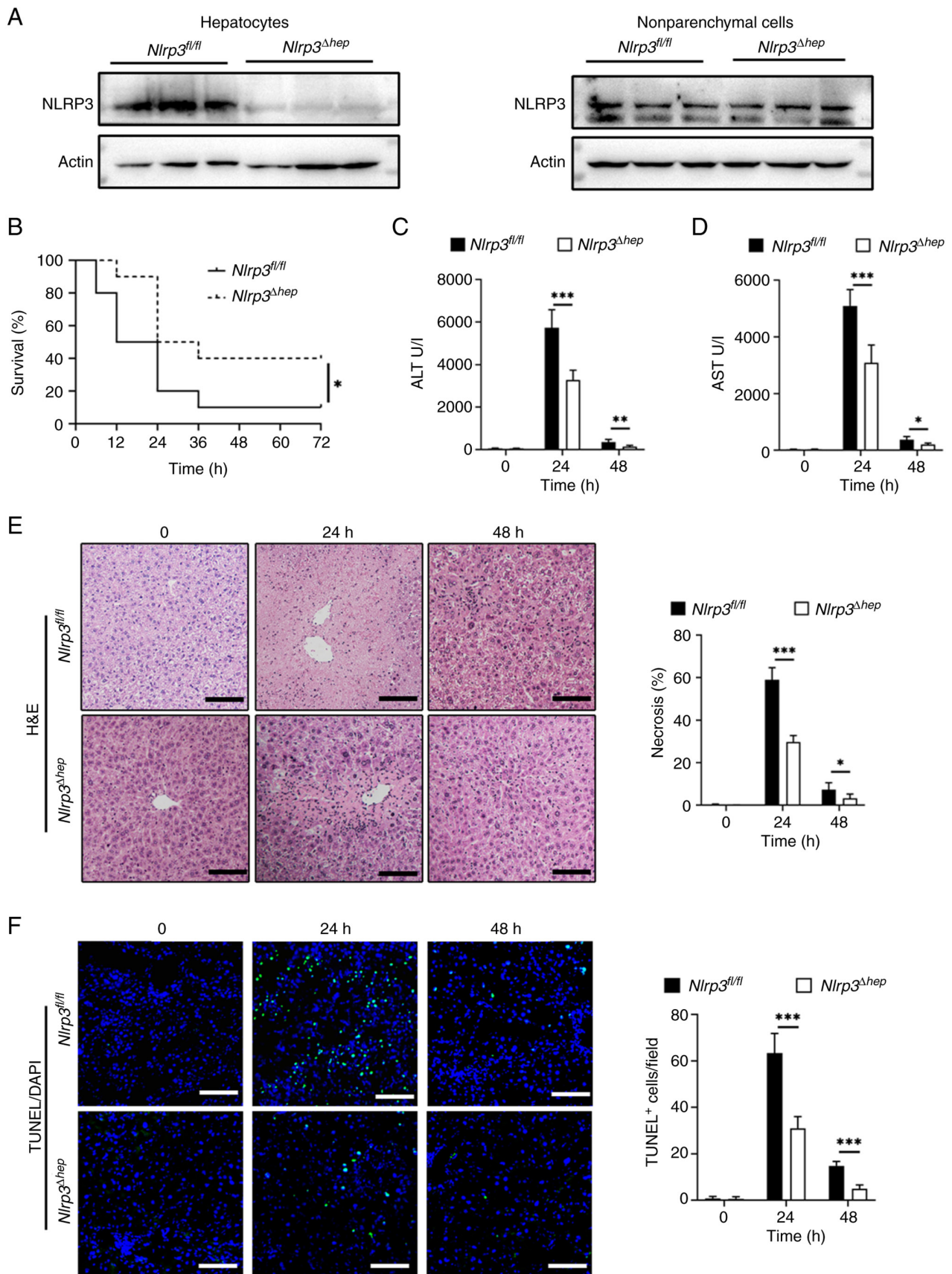


Figure 3. Hepatic NLRP3 knockout suppresses APAP-induced acute liver injury and mortality. Both *Nlrp3^{fl/fl}* and *Nlrp3^{Δhep}* mice were intraperitoneally injected with 300 mg/kg APAP (n=5). (A) NLRP3 protein expression in primary liver parenchymal cells and liver non-parenchymal cells of *NLRP3^{fl/fl}* mice and *Nlrp3^{Δhep}* mice (n=3). (B) Survival curve of *Nlrp3^{fl/fl}* and *Nlrp3^{Δhep}* mice treated with 500 mg/kg APAP (lethal dose) (n=10). Serum (C) ALT and (D) AST levels for both genotypes received 300 mg/kg APAP. (E) Representative H&E staining and the statistical quantification of hepatic necrosis. (F) Representative images of TUNEL staining and the statistical quantification of TUNEL-positive cells/field. Data are presented as the mean ± SD. *P<0.05, **P<0.01, ***P<0.001. APAP, acetaminophen; NLRP3, NLR family pyrin domain containing 3; ALT, alanine aminotransferase; AST, aspartate transaminase; *Nlrp3^{fl/fl}*, B6JNju;B6Nju-Nlrp3 (*flper*)^{tm1}/Nju mice; *Nlrp3^{Δhep}*, hepatocyte-specific *Nlrp3* knockout mice.

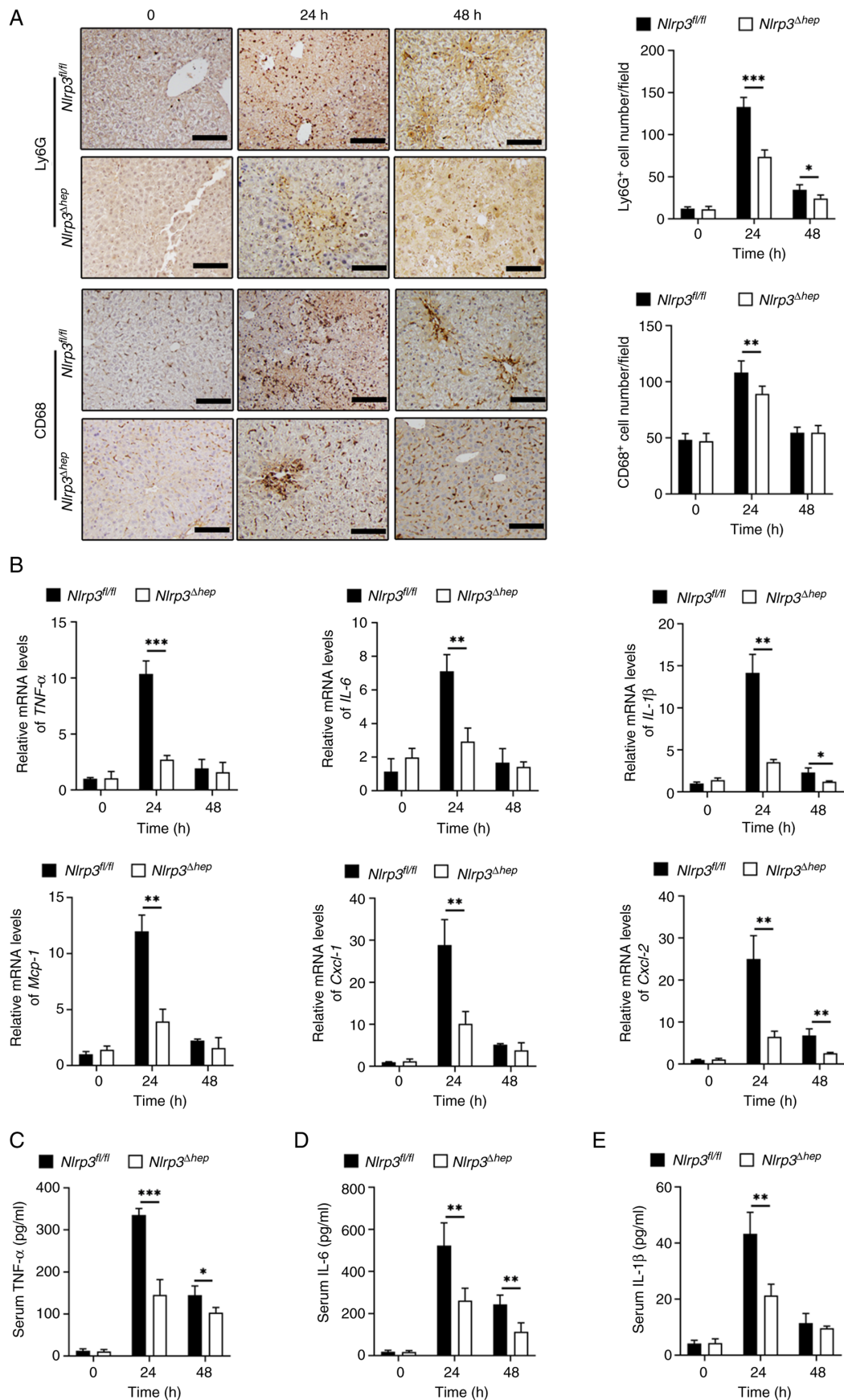


Figure 4. Hepatic NLRP3 deficiency attenuates the inflammatory reaction to APAP overdose. Both *Nlrp3^{fl/fl}* and *Nlrp3^{Δhep}* mice were intraperitoneally injected with 300 mg/kg APAP (n=5). (A) Representative hepatic Ly6G and CD68 immunohistochemical staining of liver sections and positive cell number/field were shown. (B) The relative mRNA levels of inflammatory cytokines *Tnf-α*, *Il-6*, *Il-1β* and chemokines *Mcp-1*, *Cxcl-1*, *Cxcl-2* in liver tissues were determined by RT-qPCR. ELISA analyses of the serum levels of (C) TNF-α, (D) IL-6 and (E) IL-1β. Data are presented as the mean ± SD. *P<0.05, **P<0.01, ***P<0.001. APAP, acetaminophen; NLRP3, NLR family pyrin domain containing 3; RT-qPCR, reverse transcription-quantitative PCR; *Nlrp3^{fl/fl}*, *B6JNju*; *B6NNju-Nlrp3^{flper}*^{tm1}/*Nju* mice; *Nlrp3^{Δhep}*, hepatocyte-specific *Nlrp3* knockout mice.

inhibition in APAP-induced liver injury, MCC950, an NLRP3 inhibitor, was used as previously described (34). *In vivo*, C57BL/6 mice were administered with MCC950 or PBS following APAP treatment and serum ALT, AST were evaluated at 24 and 48 h post-APAP treatment. The proportion of liver necrosis (Fig. 5A) and TUNEL-positive cell labeling (Fig. 5B) were significantly decreased with MCC950 treatment at 24 and 48 h compared with the PBS controls. Likewise, serum ALT (Fig. 5C) and AST (Fig. 5D) levels were significantly reduced in the MCC950 treated group at 24 h compared with the PBS treatment. *In vitro* experiments using AML12 cells treated with or without APAP showed that MCC950 improved cell viability, although the increase was small (Fig. 5E).

Additionally, western blotting demonstrated that 1 μ M MCC950 treatment significantly decreased the levels of the active fragments from pyroptosis-related proteins including cleaved caspase-1, cleaved IL-1 β and GSDMD-N in AML12 cells compared with the 0 μ M MCC950 control (Fig. 5F).

To further validate the association between NLRP3-mediated pyroptosis and its protective effect on AILI, DSF, a GSDMD inhibitor, was used as previously described (35,36). Mice were administered with either DSF or vehicle prior to APAP treatment. Area of liver necrosis in the DSF group was decreased compared with vehicle (Fig. 6A). The results also demonstrated a significant reduction in serum ALT/AST levels in the group treated with DSF compared with the vehicle controls. (Fig. 6C and D). Moreover, IHC revealed a significant decrease in caspase-3 positive cells at 24 and 48 h post APAP treatment compared with the vehicle controls. (Fig. 6B), which is considered an indicator of cell death. Moreover, DSF significantly decreased the levels of GSDMD-N and cleaved caspase-3 with 1 μ M DSF treatment with compared with the 0 μ M DSF control suggesting that this treatment prevented pyroptosis of AML12 cells (Fig. 6E).

Hepatic Nlrp3 deficiency promotes liver repair following APAP-induced liver injury. Evidence suggests that the timely initiation of liver regeneration is crucial for recovery from APAP-induced hepatotoxicity (6). In the present study, the regenerative capacity of *Nlrp3*^{Δhep} and *NLRP3*^{fl/fl} mice at 24 and 48 h post APAP treatment were assessed. A significant increase in the number of PCNA-positive and Ki67-positive hepatocytes in *Nlrp3*^{Δhep} mice at 24 and 48 h compared with the *Nlrp3*^{fl/fl} mice were observed (Fig. 7A).

Moreover, mRNA expression levels of *Cyclin A2* (Fig. 7B), *Cyclin D1* (Fig. 7C) and *Cyclin E1* (Fig. 7D), which are pivotal regulators of cell proliferation, were significantly increased at 24 and 48 h post APAP treatment in *Nlrp3*^{Δhep} mice compared with the *NLRP3*^{fl/fl} mice.

Furthermore, western blotting confirmed elevated protein levels of CCND1 and PCNA in *Nlrp3*^{Δhep} mice at 24 and 48 h post APAP treatment compared with the *NLRP3*^{fl/fl} mice (Fig. 7E), consistent with the aforementioned results (Fig. 7B-D). These findings suggest that hepatic NLRP3 deficiency promotes liver repair following APAP-induced liver injury.

Discussion

APAP is one of the most commonly used over-the-counter analgesics and antipyretics (37). While it demonstrates beneficial

effects when used as directed, excessive doses can lead to hepatotoxicity and dose-dependent ALF. The occurrence of AILI remains a significant challenge in clinical practice. In the present study, the activation of NLRP3 in hepatocytes following APAP overdose was demonstrated. Functionally, these findings indicate that deficiency of NLRP3 in hepatocytes protects against liver damage in mice treated with APAP, potentially by reducing inflammation and promoting hepatic restoration. Furthermore, these results suggest that this protective effect may be associated with GSDMD-mediated pyroptosis.

Pyroptosis is a form of programmed cell death that is mediated by inflammatory caspases (38,39). While it has been suggested that NLRP3-mediated pyroptosis is closely associated with acute or chronic liver injury, the role it serves in AILI remains controversial (20). Some studies have indicated that NLRP3 activation and IL-1 β maturation have little impact on APAP hepatotoxicity (40), but previous research has shown that the NLRP3/GSDMD signaling pathway serves a critical role in APAP-induced hepatocyte death (41-43). Inhibition of NLRP3-mediated pyroptosis by caveolin-1 or peroxiredoxin 3 has been shown to alleviate APAP-induced liver injury (20,44). In the present study, histopathological analysis was performed by calculating necrotic areas of liver tissue, as previously described (45-52). It was demonstrated that administration of APAP (300 mg/kg) caused severe liver injury with a time-dependent profile characterized by extensive centrilobular necrosis and elevated serum ALT and AST activities. It was also observed that NLRP3 activation was induced as early as 6 h post-APAP treatment, peaked at 12-24 h and then gradually decreased, similar to the observed time-course of liver pathology following APAP administration. Furthermore, the levels of active fragments of pyroptosis-related proteins, cleaved caspase-1, GSDMD-N and cleaved IL-1 β were increased after APAP treatment both *in vivo* and *in vitro*, indicating direct involvement of NLRP3-mediated pyroptosis in APAP hepatotoxicity.

Growing evidence suggest that Kupffer cells and neutrophil infiltration are significant in liver injury (53-55). Notably, this data showed significantly decreased liver injury in hepatocyte-specific *Nlrp3* knockout mice. Moreover, the pharmacological inhibition of NLRP3/GSDMD signaling by MCC950 or DSF had similar outcomes to those observed in *Nlrp3*^{Δhep} mice, implying its potential applications in the treatment of acetaminophen overdose.

An increasing number of previous studies have revealed that sterile inflammation is a significant factor in the pathogenesis of APAP hepatotoxicity, secondary to oxidative stress and necrotic cell death (56-58). It is recognized that the NLRP3 inflammasome serves a crucial role in initiating and sustaining sterile inflammation in various diseases (59-61). Upon exposure to stimuli, the NLRP3 inflammasome activates and cleaves caspase-1 by interacting with the apoptosis-associated speck-like protein containing a caspase recruitment domain, which leads to the maturation of IL-1 β and IL-18, ultimately exacerbating the inflammatory response (62). The NLRP3 inflammasome is implicated in the release of pro-inflammatory cytokines in APAP treated mice, and *Nlrp3* knockout mice exhibit less severe AILI and inflammation (22). Consistently, the results of the present

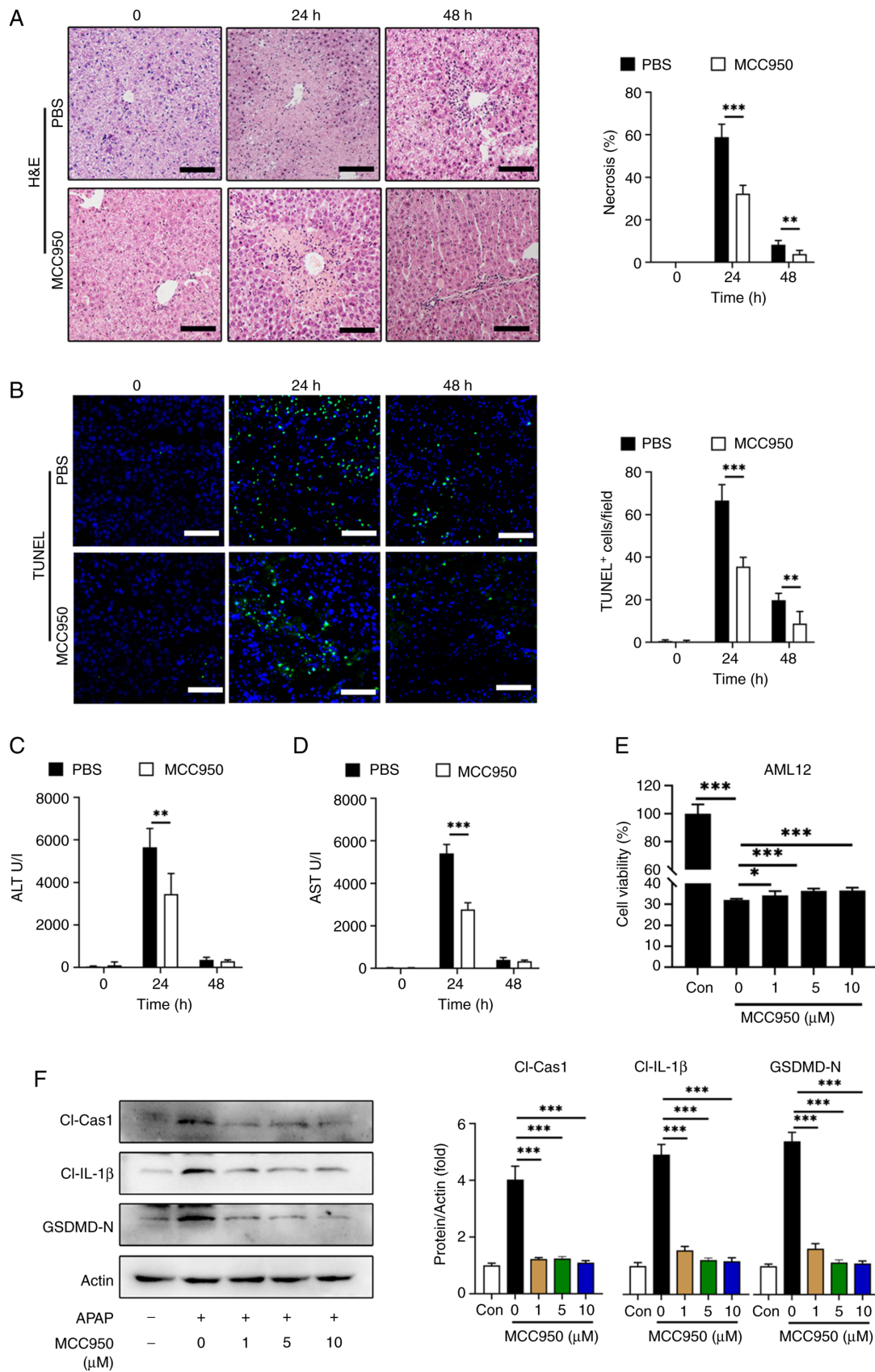


Figure 5. NLRP3 inhibitor MCC950 alleviates APAP-induced liver injury and hepatocyte pyroptosis. C57BL/6 mice were treated with MCC950 or PBS following APAP treatment ($n=5$). The therapeutic effect of MCC950 in APAP induced liver injury, with PBS treated mice as control. (A) Representative images of H&E staining and the statistical quantification of hepatic necrosis in each group. (B) Representative images of TUNEL staining and the statistical quantification of TUNEL-positive cells/field in two groups. Serum (C) ALT and (D) AST levels for two groups. (E) Viability of AML12 cells after co-treatment with APAP and different concentrations of MCC950 for 24 h. (F) Western blotting of cl-cas-1, cl-IL-1 β , GSDMD-N and the statistical quantification of each protein level in AML12 cells after co-treatment with 10 mM APAP and 0, 1, 5, 10 μ M MCC950 for 24 h. Data are presented as the mean \pm SD. * $P<0.05$, ** $P<0.01$, *** $P<0.001$. APAP, acetaminophen; NLRP3, NLR family pyrin domain containing 3; cl-cas-1, cl-caspase-1; GSDMD-N, cleaved gasdermin D N-terminal fragment; cl-IL-1 β , cleaved IL-1 β .

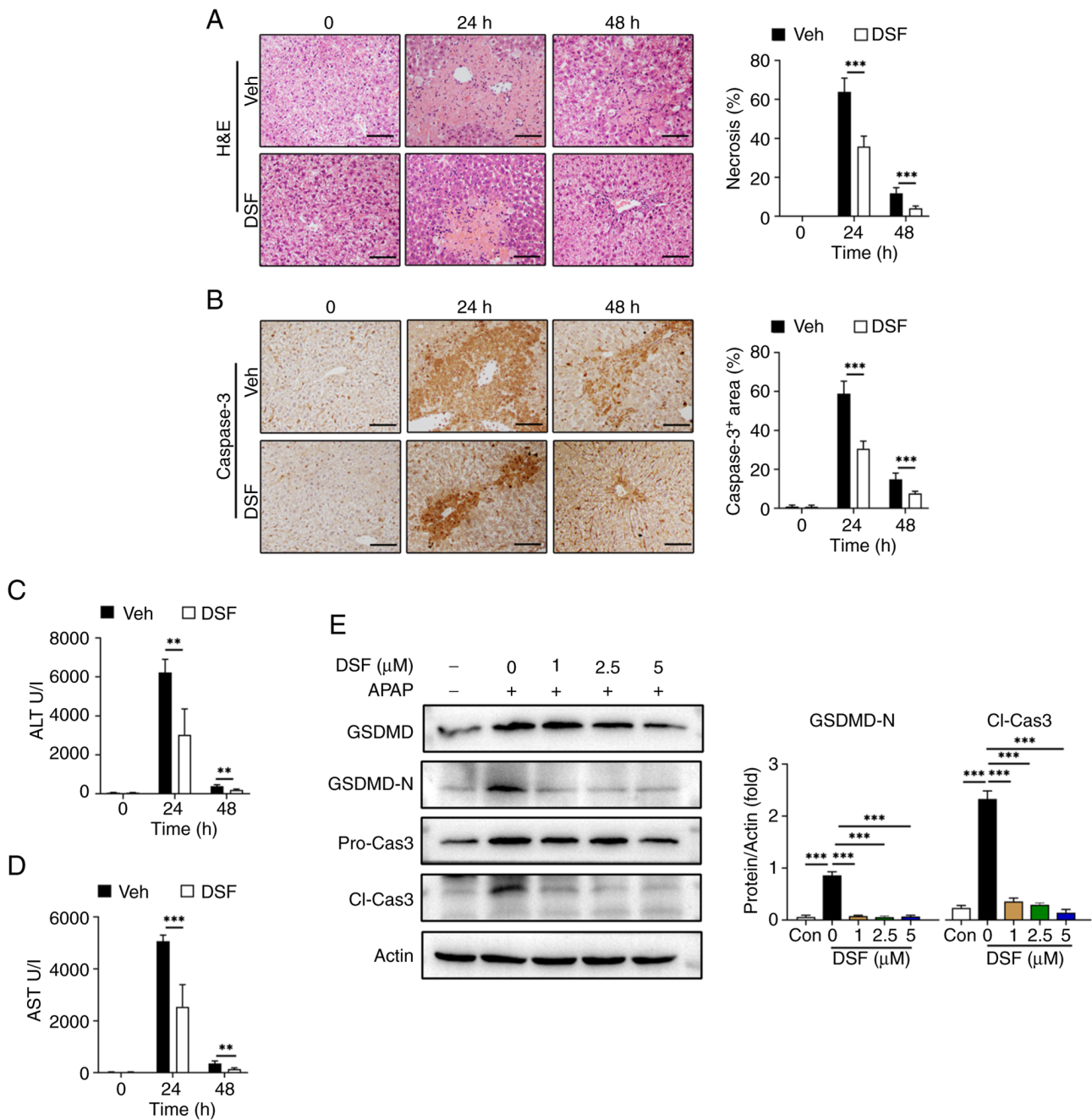


Figure 6. GSDMD inhibitor DSF mitigates APAP-induced liver injury and hepatocyte pyroptosis. C57BL/6 mice were treated with DSF or vehicle prior to APAP treatment (n=5). (A) Representative images of H&E staining and the statistical quantification of hepatic necrosis. (B) IHC staining of hepatic Caspase-3 and the statistical quantification of the positive area. Serum (C) ALT and (D) AST levels for two groups. (E) Western blotting of GSDMD-N, Pro-Cas-3/Cl-Cas-3 and the statistical quantification of each protein level in AML12 cells after co-culture with 10 mM APAP and 0, 1, 2.5, 5 μ M DSF for 24 h. Data were presented as the mean \pm SD. **P<0.01, ***P<0.001. APAP, acetaminophen; cl-cas-1, cl-caspase-1; pro-cas-1, pro-caspase-1; GSDMD, gasdermin D; GSDMD-N, cleaved GSDMD N-terminal fragment; DSF, disulfiram; IHC, immunohistochemical staining; ALT, alanine aminotransferase; AST, aspartate transaminase.

study showed significantly reduced infiltration of neutrophils (Ly6G⁺) and monocytes (CD68⁺), as well as decreased levels of pro-inflammatory cytokines and chemokines in *Nlrp3^{4hep}* mice. These findings suggest that the NLRP3 inflammasome expressed by hepatocytes might contribute to immune responses during AILI.

Previous studies have demonstrated that liver compensatory regeneration is a pivotal determinant of survival after APAP overdose, and enhancing liver regeneration has been reported to improve the final outcome of AILI (63-66).

The inflammatory response is involved in the initiation and regulation of the liver regeneration (67), but excess inflammation serves as a detrimental factor that aggravates liver damage (68). Although the NLRP3 inflammasome is known to contribute to initiating inflammation during the early stage of liver injury (43), its potential involvement in liver regeneration after APAP overdose remains unclear. A previous study has shown that dexmedetomidine promotes liver regeneration by suppressing the NLRP3 inflammasome in a partial hepatectomy model (69). Similarly, GSDMD-mediated pyroptosis

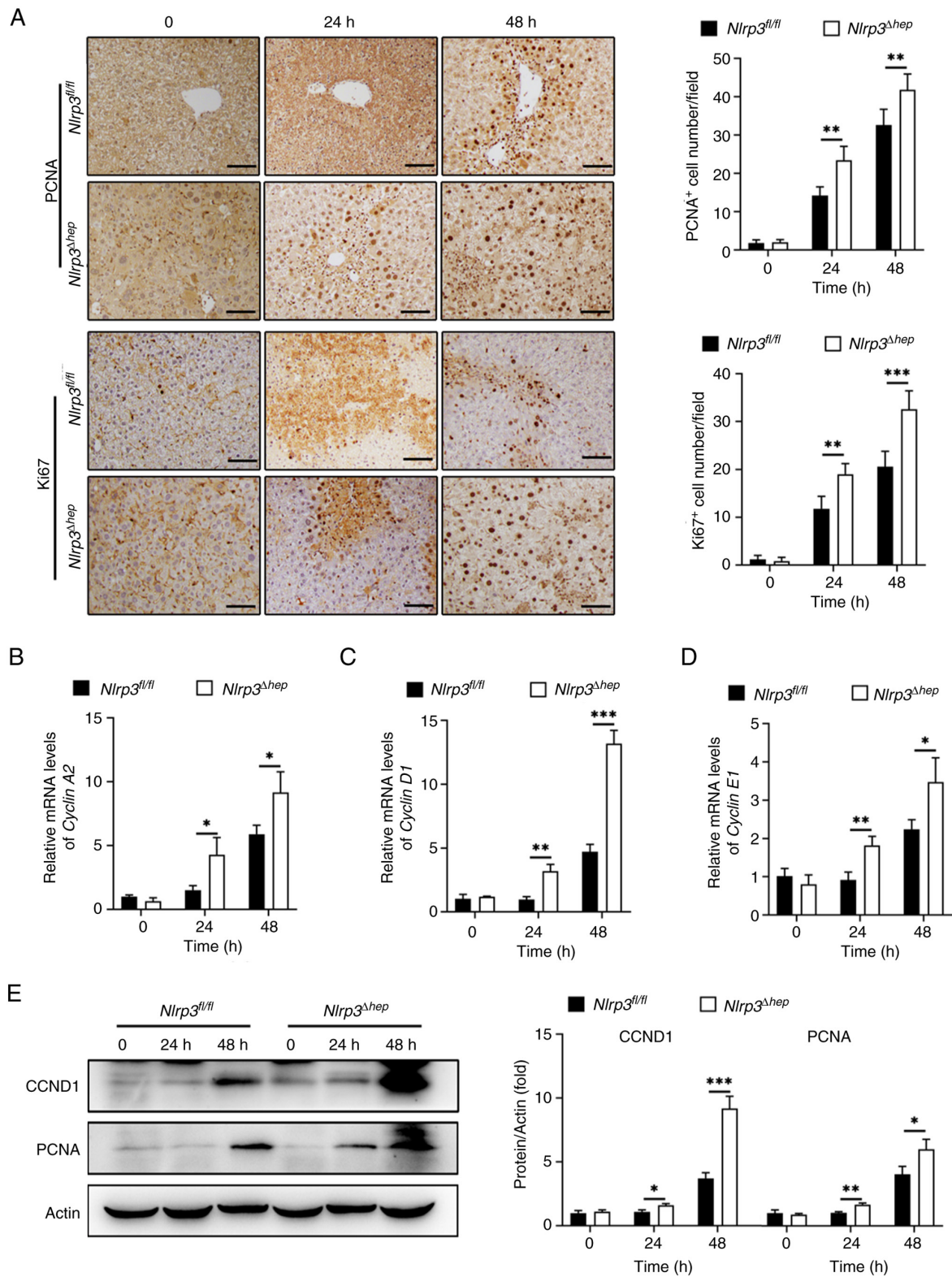


Figure 7. Hepatic NLRP3 deficiency promotes liver repair after APAP treatment. Both *Nlrp3^{fl/fl}* and *Nlrp3^{Δhep}* mice were injected intraperitoneally with 300 mg/kg APAP (n=5). (A) Representative images of hepatic PCNA and Ki67 immunohistochemical staining of liver sections and the statistical quantification of the positive cell number/field were shown. mRNA expression of mitogenic genes (B) *Cyclin A2*, (C) *Cyclin D1* and (D) *Cyclin E1* in liver tissues were determined using RT-qPCR. (E) Western blotting of CCND1 and PCNA in liver tissues and quantification of the CCND1 and PCNA protein expression in both *Nlrp3^{fl/fl}* and *Nlrp3^{Δhep}* mice. Data are presented as the mean \pm SD. * $P<0.05$, ** $P<0.01$, *** $P<0.001$. APAP, acetaminophen; NLRP3, NLR family pyrin domain containing 3; RT-qPCR, reverse transcription-quantitative PCR. *Nlrp3^{fl/fl}*, *B6JNju;B6NNju-Nlrp3 (flper)^{tm1}/Nju* mice; *Nlrp3^{Δhep}*, hepatocyte-specific *Nlrp3* knockout mice.

has been found to suppress liver regeneration using the same model (35). However, another study has revealed that NLRP3

inflammasome activation accelerates hepatocyte proliferation after AILI (70). In the present study, by utilizing hepatocyte

Nlrp3 knockout mice, it was observed that hepatocyte NLRP3 deficiency increased the number of mitotic hepatocytes and increased the expression of hepatic PCNA and CCND1 at 24 and 48 h after APAP overdose. From this it can be speculated that more hepatocytes would survive pyroptosis in the context of NLRP3 deficiency, where mitogenic genes are upregulated. However, further research is needed to elucidate the underlying mechanism.

In conclusion, the present study demonstrated that NLRP3 deficiency inhibited hepatocyte pyroptosis, alleviated inflammatory response, and promoted hepatocyte proliferation in AILI. These results identify the critical regulatory role of NLRP3-mediated pyroptosis in APAP-induced hepatotoxicity and provides novel insights into the pathological mechanisms of AILI.

Acknowledgements

Not applicable.

Funding

The present work was supported by the National Key R&D Program of China Grants (grant no. 2018YFA0109800), the Shandong Provincial Natural Science Foundation grant (grant no. ZR2022MH183) and the Shandong Provincial Youth Entrepreneurship Program for Colleges and Universities (grant no. 2022KJ148).

Availability of data and materials

The datasets used and/or analyzed during the current study are available from the corresponding author upon reasonable request.

Authors' contributions

XY, PC contributed to sample testing, data analysis and study design. XL, CY, LM and YZ contributed to sample preparation. AL and TS contributed to study design. GD directed the project, contributed to the conception and design of the work. GD had full access to all the data in the study and had final responsibility for the decision to submit for publication. XY, PC and GD confirm the authenticity of all the raw data. All authors have read and approved the final version of the manuscript.

Ethics approval and consent to participate

This study was approved by The Ethics Committee Medical College of Qingdao University (approval no. QDU-AEC-2022310).

Patient consent for publication

Not applicable.

Competing interests

The authors declare that they have no competing interests.

References

1. Gulmez SE, Larrey D, Pageaux GP, Lignot S, Lassalle R, Jové J, Gatta A, McCormick PA, Metselaar HJ, Monteiro E, *et al*: Transplantation for acute liver failure in patients exposed to NSAIDs or paracetamol (acetaminophen): The multinational case-population SALT study. *Drug Saf* 36: 135-144, 2013.
2. Larson AM, Polson J, Fontana RJ, Davern TJ, Lalani E, Hynan LS, Reisch JS, Schiødt FV, Ostapowicz G, Shakil AO, *et al*: Acetaminophen-induced acute liver failure: Results of a United States multicenter, prospective study. *Hepatology* 42: 1364-1372, 2005.
3. Gow PJ, Jones RM, Dobson JL and Angus PW: Etiology and outcome of fulminant hepatic failure managed at an Australian liver transplant unit. *J Gastroenterol Hepatol* 19: 154-159, 2004.
4. Jaeschke H, Adelusi OB, Akakpo JY, Nguyen NT, Sanchez-Guerrero G, Umbaugh DS, Ding WX and Ramachandran A: Recommendations for the use of the acetaminophen hepatotoxicity model for mechanistic studies and how to avoid common pitfalls. *Acta Pharm Sin B* 11: 3740-3755, 2021.
5. Du K, Ramachandran A and Jaeschke H: Oxidative stress during acetaminophen hepatotoxicity: Sources, pathophysiological role and therapeutic potential. *Redox Biol* 10: 148-156, 2016.
6. Bhushan B and Apte U: Liver regeneration after acetaminophen hepatotoxicity: Mechanisms and therapeutic opportunities. *Am J Pathol* 189: 719-729, 2019.
7. Jaeschke H, McGill MR and Ramachandran A: Oxidant stress, mitochondria, and cell death mechanisms in drug-induced liver injury: Lessons learned from acetaminophen hepatotoxicity. *Drug Metab Rev* 44: 88-106, 2012.
8. Jaeschke H, Williams CD, Ramachandran A and Bajt ML: Acetaminophen hepatotoxicity and repair: The role of sterile inflammation and innate immunity. *Liver Int* 32: 8-20, 2012.
9. Kubes P and Mehal WZ: Sterile inflammation in the liver. *Gastroenterology* 143: 1158-1172, 2012.
10. Bajt ML, Knight TR, Farhood A and Jaeschke H: Scavenging peroxynitrite with glutathione promotes regeneration and enhances survival during acetaminophen-induced liver injury in mice. *J Pharmacol Exp Ther* 307: 67-73, 2003.
11. Wang L, Jiao XF, Wu C, Li XQ, Sun HX, Shen XY, Zhang KZ, Zhao C, Liu L, Wang M, *et al*: Trimetazidine attenuates dexamethasone-induced muscle atrophy via inhibiting NLRP3/GSDMD pathway-mediated pyroptosis. *Cell Death Discov* 7: 251, 2021.
12. Shi J, Zhao Y, Wang K, Shi X, Wang Y, Huang H, Zhuang Y, Cai T, Wang F and Shao F: Cleavage of GSDMD by inflammatory caspases determines pyroptotic cell death. *Nature* 526: 660-665, 2015.
13. Sborgi L, Ruhl S, Mulvihill E, Pipercevic J, Heilig R, Stahlberg H, Farady CJ, Müller DJ, Broz P and Hiller S: GSDMD membrane pore formation constitutes the mechanism of pyroptotic cell death. *EMBO J* 35: 1766-1778, 2016.
14. He WT, Wan H, Hu L, Chen P, Wang X, Huang Z, Yang ZH, Zhong CQ and Han J: Gasdermin D is an executor of pyroptosis and required for interleukin-1 β secretion. *Cell Res* 25: 1285-1298, 2015.
15. Yu C, Chen P, Miao L and Di G: The Role of the NLRP3 inflammasome and programmed cell death in acute liver injury. *Int J Mol Sci* 24: 3067, 2023.
16. Yang W, Tao K, Zhang P, Chen X, Sun X and Li R: Maresin 1 protects against lipopolysaccharide/d-galactosamine-induced acute liver injury by inhibiting macrophage pyroptosis and inflammatory response. *Biochem Pharmacol* 195: 114863, 2022.
17. Han D, Kim H, Kim S, Le QA, Han SY, Bae J, Shin HW, Kang HG, Han KH, Shin J and Park HW: Sestrin2 protects against cholestatic liver injury by inhibiting endoplasmic reticulum stress and NLRP3 inflammasome-mediated pyroptosis. *Exp Mol Med* 54: 239-251, 2022.
18. Ruan S, Han C, Sheng Y, Wang J, Zhou X, Guan Q, Li W, Zhang C and Yang Y: Antcin A alleviates pyroptosis and inflammatory response in Kupffer cells of non-alcoholic fatty liver disease by targeting NLRP3. *Int Immunopharmacol* 100: 108126, 2021.
19. Liu T, Yang L, Gao H, Zhuo Y, Tu Z, Wang Y, Xun J, Zhang Q, Zhang L and Wang X: 3,4-dihydroxyphenylethyl alcohol glycoside reduces acetaminophen-induced acute liver failure in mice by inhibiting hepatocyte ferroptosis and pyroptosis. *PeerJ* 10: e13082, 2022.

20. Wang Y, Zhao Y, Wang Z, Sun R, Zou B, Li R, Liu D, Lin M, Zhou J, Ning S, *et al*: Peroxiredoxin 3 inhibits acetaminophen-induced liver pyroptosis through the regulation of mitochondrial ROS. *Front Immunol* 12: 652782, 2021.
21. Wang JC, Shi Q, Zhou Q, Zhang LL, Qiu YP, Lou DY, Zhou LQ, Yang B, He QJ, Weng QJ and Wang JJ: Sapindolide A alleviates acetaminophen-induced acute liver injury by inhibiting NLRP3 inflammasome activation in macrophages. *Acta Pharmacol Sin* 43: 2016-2025, 2022.
22. Imaeda AB, Watanabe A, Sohail MA, Mahmood S, Mohamadnejad M, Sutterwala FS, Flavell RA and Mehal WZ: Acetaminophen-induced hepatotoxicity in mice is dependent on Tlr9 and the Nalp3 inflammasome. *J Clin Invest* 119: 305-314, 2009.
23. Zhang C, Feng J, Du J, Zhuo Z, Yang S, Zhang W, Wang W, Zhang S, Iwakura Y, Meng G, *et al*: Macrophage-derived IL-1 α promotes sterile inflammation in a mouse model of acetaminophen hepatotoxicity. *Cell Mol Immunol* 15: 973-982, 2018.
24. Chen CJ, Kono H, Golenbock D, Reed G, Akira S and Rock KL: Identification of a key pathway required for the sterile inflammatory response triggered by dying cells. *Nat Med* 13: 851-856, 2007.
25. Li M, Sun X, Zhao J, Xia L, Li J, Xu M, Wang B, Guo H, Yu C, Gao Y, *et al*: CCL5 deficiency promotes liver repair by improving inflammation resolution and liver regeneration through M2 macrophage polarization. *Cell Mol Immunol* 17: 753-764, 2020.
26. Wang B, Li J, Jiao J, Xu M, Luo Y, Wang F, Xia Q, Gao Y, Feng Y, Kong X and Sun X: Myeloid DJ-1 deficiency protects acetaminophen-induced acute liver injury through decreasing inflammatory response. *Aging (Albany NY)* 13: 18879-18893, 2021.
27. Wen Y, Feng D, Wu H, Liu W, Li H, Wang F, Xia Q, Gao WQ and Kong X: Defective initiation of liver regeneration in osteopontin-deficient mice after partial hepatectomy due to insufficient activation of IL-6/Stat3 Pathway. *Int J Biol Sci* 11: 1236-1247, 2015.
28. Ni HM, Du K, You M and Ding WX: Critical role of FoxO3a in alcohol-induced autophagy and hepatotoxicity. *Am J Pathol* 183: 1815-1825, 2013.
29. Luan X, Chen P, Li Y, Yuan X, Miao L, Zhang P, Cao Q, Song X and Di G: TNF- α /IL-1 β -licensed hADSCs alleviate cholestatic liver injury and fibrosis in mice via COX-2/PGE2 pathway. *Stem Cell Res Ther* 14: 100, 2023.
30. Livak KJ and Schmittgen TD: Analysis of relative gene expression data using real-time quantitative PCR and the 2(-Delta Delta C(T)) Method. *Methods* 25: 402-408, 2001.
31. Xu J, Chen P, Yu C, Shi Q, Wei S, Li Y, Qi H, Cao Q, Guo C, Wu X and Di G: Hypoxic bone marrow mesenchymal stromal cells-derived exosomal miR-182-5p promotes liver regeneration via FOXO1-mediated macrophage polarization. *FASEB J* 36: e22553, 2022.
32. Wei S, Li Z, Shi Q, Luan X, Yuan X, Li Y, Guo C, Wu X, Shi C and Di G: Collagen-binding vascular endothelial growth factor (CBD-VEGF) promotes liver regeneration in murine partial hepatectomy. *Mol Med Rep* 26: 326, 2022.
33. Triantafyllou E, Pop OT, Possamai LA, Wilhelm A, Liaskou E, Singanayagam A, Bernsmeier C, Khamri W, Petts G, Dargue R, *et al*: MerTK expressing hepatic macrophages promote the resolution of inflammation in acute liver failure. *Gut* 67: 333-347, 2018.
34. Mridha AR, Wree A, Robertson AAB, Yeh MM, Johnson CD, Van Rooyen DM, Haczeiny F, Teoh NC, Savard C, Ioannou GN, *et al*: NLRP3 inflammasome blockade reduces liver inflammation and fibrosis in experimental NASH in mice. *J Hepatol* 66: 1037-1046, 2017.
35. Lv X, Chen J, He J, Hou L, Ren Y, Shen X, Wang Y, Ji T and Cai X: Gasdermin D-mediated pyroptosis suppresses liver regeneration after 70% partial hepatectomy. *Hepatol Commun* 6: 2340-2353, 2022.
36. Hu JJ, Liu X, Xia S, Zhang Z, Zhang Y, Zhao J, Ruan J, Luo X, Lou X, Bai Y, *et al*: FDA-approved disulfiram inhibits pyroptosis by blocking gasdermin D pore formation. *Nat Immunol* 21: 736-745, 2020.
37. Chowdhury A, Nabila J, Adelusi Temitope I and Wang S: Current etiological comprehension and therapeutic targets of acetaminophen-induced hepatotoxicity. *Pharmacol Res* 161: 105102, 2020.
38. Kovacs SB and Miao EA: Gasdermins: Effectors of pyroptosis. *Trends Cell Biol* 27: 673-684, 2017.
39. Broz P and Dixit VM: Inflammasomes: Mechanism of assembly, regulation and signalling. *Nat Rev Immunol* 16: 407-420, 2016.
40. Williams CD, Farhood A and Jaeschke H: Role of caspase-1 and interleukin-1 β in acetaminophen-induced hepatic inflammation and liver injury. *Toxicol Appl Pharmacol* 247: 169-178, 2010.
41. Cai C, Huang H, Whelan S, Liu L, Kautza B, Luciano J, Wang G, Chen G, Stratimirovic S, Tsung A, *et al*: Benzyl alcohol attenuates acetaminophen-induced acute liver injury in a Toll-like receptor-4-dependent pattern in mice. *Hepatology* 60: 990-1002, 2014.
42. Yu Y, Zhou S, Wang Y, Di S, Wang Y, Huang X and Chen Y: Leonurine alleviates acetaminophen-induced acute liver injury by regulating the PI3K/AKT signaling pathway in mice. *Int Immunopharmacol* 120: 110375, 2023.
43. Gao Z, Zhan H, Zong W, Sun M, Linghu L, Wang G, Meng F and Chen M: Salidroside alleviates acetaminophen-induced hepatotoxicity via Sirt1-mediated activation of Akt/Nrf2 pathway and suppression of NF- κ B/NLRP3 inflammasome axis. *Life Sci* 327: 121793, 2023.
44. Jiang X, Li Y, Fu D, You T, Wu S, Xin J, Wen J, Huang Y and Hu C: Caveolin-1 ameliorates acetaminophen-aggravated inflammatory damage and lipid deposition in non-alcoholic fatty liver disease via the ROS/TXNIP/NLRP3 pathway. *Int Immunopharmacol* 114: 109558, 2023.
45. Xu L, Yang Y, Jiang J, Wen Y, Jeong JM, Emontzpohl C, Atkins CL, Kim K, Jacobsen EA, Wang H and Ju C: Eosinophils protect against acetaminophen-induced liver injury through cyclooxygenase-mediated IL-4/IL-13 production. *Hepatology* 77: 456-465, 2023.
46. Chen L, Dong J, Liao S, Wang S, Wu Z, Zuo M, Liu B, Yan C, Chen Y, He H, *et al*: Loss of Sam50 in hepatocytes induces cardiolipin-dependent mitochondrial membrane remodeling to trigger mtDNA release and liver injury. *Hepatology* 76: 1389-1408, 2022.
47. Gao RY, Wang M, Liu Q, Feng D, Wen Y, Xia Y, Colgan SP, Eltzschig HK and Ju C: Hypoxia-Inducible Factor-2 α reprograms liver macrophages to protect against acute liver injury through the production of interleukin-6. *Hepatology* 71: 2105-2117, 2020.
48. Chen Y, Liu K, Zhang J, Hai Y, Wang P, Wang H, Liu Q, Wong CCL, Yao J, Gao Y, *et al*: c-Jun NH2-Terminal protein kinase phosphorylates the Nrf2-ECH Homology 6 domain of nuclear factor erythroid 2-Related Factor 2 and downregulates cytoprotective genes in acetaminophen-induced liver injury in mice. *Hepatology* 71: 1787-1801, 2020.
49. Park S, Park J, Kim E and Lee Y: The Capicua/ETS translocation variant 5 axis regulates liver-resident memory CD8(+) T-Cell development and the pathogenesis of liver injury. *Hepatology* 70: 358-371, 2019.
50. Chen D, Ni HM, Wang L, Ma X, Yu J, Ding WX and Zhang L: p53 Up-regulated modulator of apoptosis induction mediates acetaminophen-induced necrosis and liver injury in mice. *Hepatology* 69: 2164-2179, 2019.
51. Sun Y, Li TY, Song L, Zhang C, Li J, Lin ZZ, Lin SC and Lin SY: Liver-specific deficiency of unc-51 like kinase 1 and 2 protects mice from acetaminophen-induced liver injury. *Hepatology* 67: 2397-2413, 2018.
52. Zhang C, Lin J, Zhen C, Wang F, Sun X, Kong X and Gao Y: Amygdalin protects against acetaminophen-induced acute liver failure by reducing inflammatory response and inhibiting hepatocyte death. *Biochem Biophys Res Commun* 602: 105-112, 2022.
53. Pu JL, Huang ZT, Luo YH, Mou T, Li TT, Li ZT, Wei XF and Wu ZJ: Fisetin mitigates hepatic ischemia-reperfusion injury by regulating GSK3 β /AMPK/NLRP3 inflammasome pathway. *Hepatobiliary Pancreat Dis Int* 20: 352-360, 2021.
54. Huang Z, Mou T, Luo Y, Pu X, Pu J, Wan L, Gong J, Yang H, Liu Y, Li Z, *et al*: Inhibition of miR-450b-5p ameliorates hepatic ischemia/reperfusion injury via targeting CRYAB. *Cell Death Dis* 11: 455, 2020.
55. Chen YX, Sato M, Kawachi K and Abe Y: Neutrophil-mediated liver injury during hepatic ischemia-reperfusion in rats. *Hepatobiliary Pancreat Dis Int* 5: 436-442, 2006.
56. James LP, Simpson PM, Farrar HC, Kearns GL, Wasserman GS, Blumer JL, Reed MD, Sullivan JE and Hinson JA: Cytokines and toxicity in acetaminophen overdose. *J Clin Pharmacol* 45: 1165-1171, 2005.
57. Shen K, Chang W, Gao X, Wang H, Niu W, Song L and Qin X: Depletion of activated hepatic stellate cell correlates with severe liver damage and abnormal liver regeneration in acetaminophen-induced liver injury. *Acta Biochim Biophys Sin (Shanghai)* 43: 307-315, 2011.

58. Woolbright BL, Nguyen NT, McGill MR, Sharpe MR, Curry SC and Jaeschke H: Generation of pro-and anti-inflammatory mediators after acetaminophen overdose in surviving and non-surviving patients. *Toxicol Lett* 367: 59-66, 2022.
59. Toldo S, Mezzaroma E, Buckley LF, Potere N, Di Nisio M, Biondi-Zoccai G, Van Tassell BW and Abbate A: Targeting the NLRP3 inflammasome in cardiovascular diseases. *Pharmacol Ther* 236: 108053, 2022.
60. Takahashi M: NLRP3 inflammasome as a key driver of vascular disease. *Cardiovasc Res* 118: 372-385, 2022.
61. Sharma BR and Kanneganti TD: NLRP3 inflammasome in cancer and metabolic diseases. *Nat Immunol* 22: 550-559, 2021.
62. Kelley N, Jeltama D, Duan Y and He Y: The NLRP3 Inflammasome: An overview of mechanisms of activation and regulation. *Int J Mol Sci* 20: 3328, 2019.
63. Nejak-Bowen KN and Monga SP: Beta-catenin signaling, liver regeneration and hepatocellular cancer: Sorting the good from the bad. *Semin Cancer Biol* 21: 44-58, 2011.
64. Donahower BC, McCullough SS, Hennings L, Simpson PM, Stowe CD, Saad AG, Kurten RC, Hinson JA and James LP: Human recombinant vascular endothelial growth factor reduces necrosis and enhances hepatocyte regeneration in a mouse model of acetaminophen toxicity. *J Pharmacol Exp Ther* 334: 33-43, 2010.
65. Schmidt LE and Dalhoff K: Alpha-fetoprotein is a predictor of outcome in acetaminophen-induced liver injury. *Hepatology* 41: 26-31, 2005.
66. Hu B and Colletti LM: Stem cell factor and c-kit are involved in hepatic recovery after acetaminophen-induced liver injury in mice. *Am J Physiol Gastrointest Liver Physiol* 295: G45-G53, 2008.
67. Hu C, Wu Z and Li L: Mesenchymal stromal cells promote liver regeneration through regulation of immune cells. *Int J Biol Sci* 16: 893-903, 2020.
68. Lazcanoiturburu N, García-Sáez J, González-Corrado C, Roncero C, Sanz J, Martín-Rodríguez C, Valdecantos MP, Martínez-Palacián A, Almalé L, Bragado P, *et al*: Lack of EGFR catalytic activity in hepatocytes improves liver regeneration following DDC-induced cholestatic injury by promoting a pro-restorative inflammatory response. *J Pathol* 258: 312-324, 2022.
69. Lv M, Zeng H, He Y, Zhang J and Tan G: Dexmedetomidine promotes liver regeneration in mice after 70% partial hepatectomy by suppressing NLRP3 inflammasome not TLR4/NFκB. *Int Immunopharmacol* 54: 46-51, 2018.
70. Shi L, Zhang S, Huang Z, Hu F, Zhang T, Wei M, Bai Q, Lu B and Ji L: Baicalin promotes liver regeneration after acetaminophen-induced liver injury by inducing NLRP3 inflammasome activation. *Free Radic Biol Med* 160: 163-177, 2020.



Copyright © 2024 Yuan et al. This work is licensed under a Creative Commons Attribution-NonCommercial-NoDerivatives 4.0 International (CC BY-NC-ND 4.0) License.